MATCHED MEYER NEURAL WAVELETS FOR CLINICAL AND EXPERIMENTAL ANALYSIS OF AUDITORY AND VISUAL EVOKED POTENTIALS

V. J. Samar[1,5] H. Begleiter[2] J. O. Chapa[3] M. R. Raghuveer[4] M. Orlando[5] D. Chorlian[2]

1. National Technical Institute for the Deaf, Rochester Institute of Technology, Rochester, NY 14623
phone: 716-475-6338, fax 716-475-6500, vjsncr@rit.edu
2. Department of Psychiatry, State University of New York Health Science Center, Brooklyn, NY 11203
3. Hanscom Air Force Base, Code ESC/AW, Hanscom AFB01731, Massachussetes 01731
4. Electrical Engineering Department, Rochester Institute of Technology, Rochester, NY 14623
5. Otolaryngology Division, University of Rochester Medical Center, Rochester, NY 14620

ABSTRACT

The wavelet transform provides a time-scale analysis that permits flexible pattern recognition, component identification, and detection of transients for time-varying neural signals such as the EEG, event-related potentials, neuromagnetic signals, and other neural signals and images. Many future applications to neural signals will benefit from choosing a mother wavelet that mimics neural waveform features. We use a recently developed algorithm to design physiologically realistic orthonormal Meyer wavelets, including 1) a wavelet that matches the prominent IV-V complex of the auditory brainstem evoked response used widely for clinical evaluation of hearing loss, and 2) a wavelet that matches ERPs containing prominent P300 components from control and alcoholic subjects. We also compare the relative naturalness of dyadic decompositions that use matched Meyer wavelets, the Haar wavelet, and Daubechies D4 wavelet. Designer neural wavelets have broad potential to customize and improve neurometric imaging and clinical neurodiagnosis of sensory and cognitive dysfunction.

1 INTRODUCTION

The wavelet transform (WT) has attractive properties for analyzing and efficiently storing neuroelectric and neuromagnetic signals and images, including variable measurement resolution matched to the scale of waveform features, computational simplicity and speed, excellent compression capability, and perfect reversibility for precise and specialized waveform filter design [1].

The core element in a wavelet analysis is the mother wavelet, a localized time-domain function satisfying certain admissibility conditions [2]. In the WT of a time-varying neural waveform $s(t)$, the mother wavelet $g(t)$ is scaled by a and translated in time by b to form a wavelet family, and the inner products of this family with the waveform are taken as in (1).

If orthonormal, the wavelet may be used in a multiresolution analysis (MRA), where an n- sample waveform is decomposed into an efficient set of n orthonormal wavelet bases at discrete time scales, $a = 2^j$, and translations, $b = 2^j k$, for j,k integers, using a simple pyramidal filter scheme of computational complexity that is merely $O(n)$ [3].

$$W(a,b) = \frac{1}{\sqrt{a}} \int_{t=-\infty}^{\infty} s(t) g^* \left(\frac{t-b}{a} \right) dt \quad (1)$$

Zeroing or manipulating some of the wavelet coefficients in (1) prior to waveform reconstruction allows precise filtering of neural waveforms for experimental and diagnostic purposes. Discarding zero, near zero, or application-irrelevant coefficients in MRAs of neural signals can yield impressive lossy compression ratios [4].

Besides the appeal of the WT as a mathematical tool for neural waveform decomposition, there is now evidence that the brain accomplishes aspects of sensory-perceptual construction by performing its own WT on sensorineural signals [9]. Wavelet representations, then, may play a basic role in the representational functions of the central nervous system. Hence, wavelets may be physiologically natural basis functions that are optimally suited to study biologically important neural functions and to satisfy the ubiquitous need of neuroscientists and clinicians to decompose neural signals into meaningful components.

The WT has been applied successfully to neural waveform analysis problems such as detection of epileptic activity [5], denoising of single-trial event-related potentials (ERP) [6], prediction of human signal detection performance from ERPs [7], and identification of scale-specific visual evoked response correlates of retinal degeneration [8]. Future applications will benefit by using wavelets optimally designed to analyze neural signals. In this paper we illustrate a method of designing Meyer wavelets matched to neural waveform features.

1.1 Rationale for Matched Neural Wavelets

Many neural signals are of interest to the neuroscience and neuroclinical communities, each exhibiting characteristic time-dependent spectral and waveshape properties. These include electroencephalographic (EEG) and magneto-encephalographic (MEG) signals, epileptic spikes, state-related EEG spindles, sensory evoked potentials, intra-cranial unit recordings, and so on.

Any wavelet, regardless of its shape, can decompose such neural signals into energy distributions that localize waveform information in time and scale (frequency),

parceled out into overlapping waveform pieces that mimic the mother wavelet in the time domain. However, if the goal of neural waveform analysis is to identify specific neural events or components, it is advantageous to choose wavelets that match the shapes of the signals of interest.

The wavelet that most closely resembles the waveshape of a neural signal is the best scale-independent analyzing function for that signal in a matched filtering sense. Wavelets that are poor shape matches to a waveform or component will tend to produce more distributed energy patterns, complicating the detection, classification, and estimation of the signal of interest.

An important potential application of neural wavelets is in statistical estimation models designed to efficiently separate and measure specific ERP components that may partially overlap in time or frequency. Recently, a statistical wavelet model of this sort has been presented by Raz and Turetsky [4]. In principle, the particular wavelet used in such models determines the robustness of component separation and the extent of acheivable data compression. Wavelets that match the general spectral properties of ERPs and the particular spectral properties of individual components will typically be the most efficient ones to use in such component identification models.

1.2 Matching Algorithm

Previously, wavelets used in studies of neural signals have been based on standard mathematical functions or recursive algorithms like Daubechies' algorithm, with no attempt to directly match wavelets to specific neural signals. Chapa and Raghuveer [10] recently derived an algorithm that designs Meyer wavelets to match specified band-limited signals as closely as possible in a least squares sense. The algorithm can design Meyer wavelets that closely match nearly any real neural signal of interest to the neuroscience and neuroclinical communities.

The Chapa and Raghuveer algorithm uses samples of $S(\omega)$, the Fourier transform of signal $s(t)$, to determine a function $G(\omega)$, the Fourier transform of wavelet $g(t)$, such that $|G(\omega)|^2$ is close to $|S(\omega)|^2$ in a least squares sense while satisfying all requirements for the energy spectrum density of Meyer wavelets. The group delay of $G(\omega)$ is also matched to that of $S(\omega)$ in a least squares sense. A scaling function and impulse responses for filter implementation are also obtained.

Raghuveer and Chapa [11] give the closed form of the magnitude matching algorithm as:

$$A(\omega) = C/2 + [B(\omega) - B(2\pi - \omega) - B(2\omega) + B(4\pi - 2\omega)]/2, \quad (2)$$

where $C = \frac{1}{\pi}\int_{2\pi/3}^{8\pi/3} B(\omega)d\omega$, $A(\omega) = |G(\omega)|^2$, and $B(\omega) = |S(\omega)|^2$, for $2\pi/3 \le \omega \le 4\pi/3$. For $4\pi/3 \le \omega \le 8\pi/3$, use $A(\omega) = A(2\pi - \omega/2)$.

Phase matching minimizes the error function in (3), subject to constraints on the group delay for band-limited wavelets. See Chapa and Raghuveer [10] for details.

$$\gamma_\Omega = \sum_{n=-N/2}^{N/2-1}\left[\Omega(n)(\Gamma_s(n) - \Gamma_g(n))\right]^2 \quad (3)$$

where $\Omega(n)$ is a normalized weighting function that limits the phase match to the passband $2\pi/3 \le |\omega| \le 8\pi/3$, and $\Gamma_S(n)$ and $\Gamma_g(n)$ are the signal and wavelet group delays, respectively.

2 SAMPLE MATCHED NEURAL WAVELETS

We focus on clinically relevant auditory and visual evoked potentials (EP), namely the auditory brainstem evoked response (ABER) used widely to evaluate hearing loss and brainstem integrity, and the visual odd-ball EP containing a P300 component used to evaluate cognitive processing.

2.1 Matched ABER Wavelet

The ABER reflects neural activity in the auditory pathway from cochlea to primary auditory cortex, developing within 10 milliseconds after auditory stimulation. Figure 1 shows ABERs from routine clinical evaluations of four adult normal-hearing patients. Each ABER is an average based on 2000 click stimuli. The six typical positive peaks are visible in each ABER, including the prominent IV-V complex used routinely in clinical evaluations.

We isolated the IV-V component complex in the rectangle, zero padded on both sides and fit an orthogonal Meyer wavelet to it. This wavelet is superimposed on the original ABER in Figure 1a. The ABER IV-V wavelet tracks the contours of the major positive crest and the characteristic deep negative trough following it quite well.

Figures 1b-1d show scaled versions of the same wavelet superimposed on the other three ABERs. The close fits indicate good shape generalization from patient to patient. These examples also show that the IV-V complex undergoes substantial time scaling from patient to patient. Up to 13% variation in time scaling is apparent. Due to its natural scaling property, the continuous WT of these ABERs, using the ABER 1 wavelet, would contain a peak in the time-scale plane at the right scale and time lag for each ABER IV-V complex.

Properly matched Meyer ABER wavelets will generally provide the most reliable and distinct identification of their target component, regardless of how the component's scale varies over patients, conditions, or trials. Such a wavelet might be used, for example, in simple pattern recognition algorithms to reliably locate similarly shaped instances of the IV-V component in noisy recordings from the same subject, independent of inter-recording variability in the scale of the component.

Increased precision due to shape matching will also improve the high noise performance of more sophisticated wavelet and wavelet-packet based component identification algorithms [4], suggesting a clear clinical application of matched neural wavelets for detecting and identifying low stimulus intensity ABER components in automated

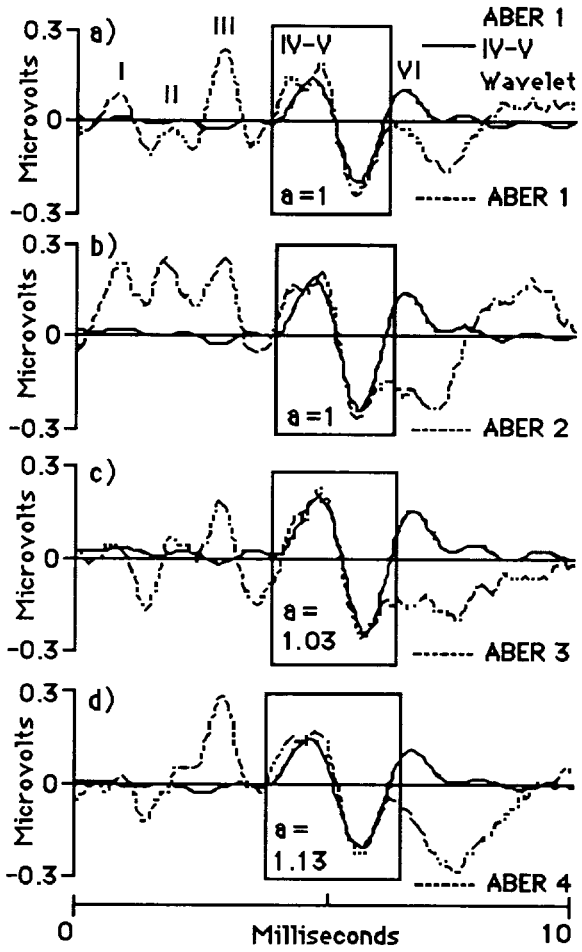

Figure 1. ABERs of 4 patients (80 dB NHL clicks). Scaling coefficient "a" indicates proportionate scaling relative to ABER 1.

audiometric threshold evaluation algorithms. Customized ABER wavelets can be incorporated into software to improve hearing assessment in the universal newborn auditory screening programs now being implemented in the United States in response to the National Institutes of Health Consensus Panel's 1993 recommendations. Generally, matched wavelets will benefit the study of auditory system function and hearing loss evaluation in infants and adults by improving the characterization of ABER responses.

2.2 Matched P300-ERP Wavelet

Figure 2b shows a Meyer wavelet matched to the group-averaged cognitive Pz P300-ERP. The P300-ERP wavelet tracks the dominant low frequency P300 component well.

2.2.1 Comparative ERP Wavelet Decompositions

Figure 2c shows multiresolution representations (MRR) associated with typical 5-level MRA wavelet decompositions of the averaged Pz P300-ERP using the matched P300-ERP wavelet, Haar wavelet, and Daubechies D4 wavelet. MRRs are sequences of successively lower resolutions of the ERP obtained by removing successive levels of high frequency detail (detail functions) by passing the ERP through wavelet based filters at successively larger dyadic scales. Clearly, the Haar and the Daubechies D4 MRRs preserve the physiologically unnatural shape properties of their wavelet basis functions up to the highest level of resolution in their MRRs.

A general shape mismatch between the ERP and the wavelet basis functions used to analyze it will tend to delocalize waveform details at specific scales of activity, dispersing energy more widely in the time-scale plane than matched wavelets. Consequently, naturally band-limited ERP components will be more concisely partitioned by a matched, physiologically natural wavelet.

The dispersive effect of shape mismatch is evident in Figure 2c. For the matched Meyer P300-ERP wavelet, the match between the MRR and the high resolution ERP is essentially complete at the level 4 resolution for the P300 component. The P1-N1-P2-N2 component complex is absent at the level 4 resolution, but appears essentially complete at the level 3 resolution, just one dyadic scale step more. This shows a neat separation into distinct, localized scales of the information associated with the P300 component and the P1-N1-P2-N2 complex, respectively. By contrast, the Haar and Daubechies MRRs tend to confound and misrepresent the P300 and the P1-N1-P2-N2 complex over several different scales.

2.2.2 Localization of Clinically Relevant Group Differences

To demonstrate that wavelet analyses can localize functionally meaningful effects in ERP data sets, we computed a 5-level MRA on each of 306 ERPs obtained in a visual odd-ball paradigm [12]. Subjects (25 controls and 26 alcoholics) produced ERPs at left and right hemisphere parietal sites (P3 and P4) in response to a rare visual target (an "X"), rare novel shapes, and a frequent standard shape (a square). MRA coefficients for these ERPs were analyzed in three 4-way repeated measures analyses of variance (ANOVA), one for the level 5 low resolution signal and one each for the levels 5 and 4 detail functions (factorial design: Group X Hemisphere X Stimulus Type X Coefficient Sequence). These three coefficient sets nominally reflect ERP frequencies in the .02-4 Hz (delta), 4-8 Hz (theta), and 8-16 Hz (alpha) ranges, respectively. The level 5 detail function contributed energy maximally to the P300, while the level 4 detail function primarily determined the P1-N1-P2-N2 complex.

The level 5 low resolution ANOVA produced no significant group effects. A significant Group X Coefficient Sequence interaction was found for each detail function: Level 5, $F(13,637)= 2.42$, $p<.0035$; Level 4, $F(29,1421)= 2.38$, $p<.0001$. Figure 3 shows the sources of these interactions graphically. The bar plots show the numerical difference between the control and alcoholic groups in the average magnitudes (absolute values) of their wavelet coefficients at each translation (time step). The superimposed grand average ERP shows that the significant group differences at level 5 (4-8 Hz theta) occurred within the span of the P300, consistent with earlier P300 studies [12], while the significant group differences at Level 4 (8-16 Hz alpha) occured primarily

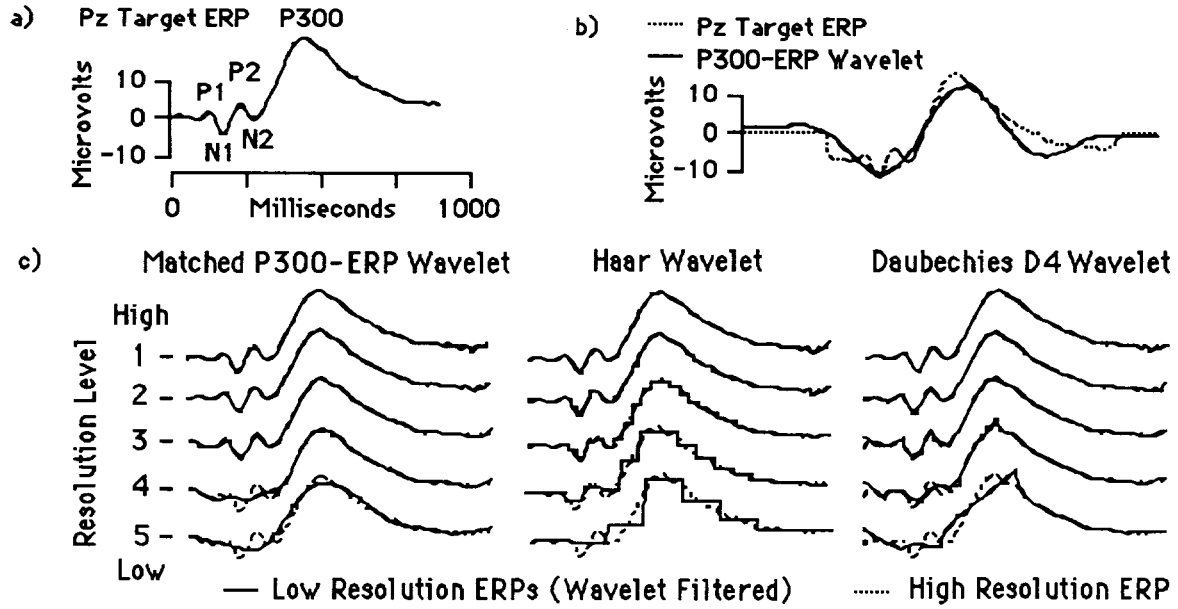

Figure 2. a) Group Averaged (16 normal subjects) Pz ERP to rare targets in a visual P300 experiment (see [12] for recording details); b) Fitted P300-ERP Wavelet; c) MRRs using matched P300-ERP, Haar, and Daubechies D4 wavelets.

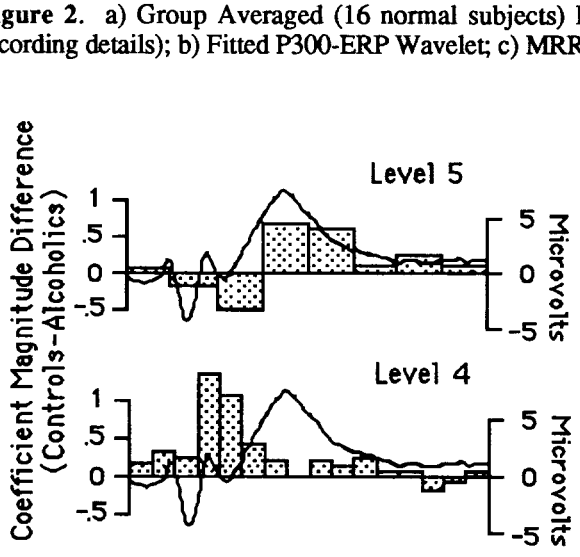

Figure 3. Group coefficient magnitude difference plots for detail functions 4 (8-16 Hz alpha) and 5 (4-8 Hz theta). Grand average ERP superimposed for time localization.

around the latter half of the P1-N1-P2-N2 complex. Differences in the P1-N1-P2-N2 complex have not been identified previously by standard peak analysis. These effects at distinct waveform scales may index distinct neural mechanisms related to alcoholism.

3. CONCLUSION

We have illustrated the construction of matched Meyer wavelets for auditory and visual neural waveforms, and have demonstrated that MRAs using such wavelets achieve a physiologically natural decomposition of ERPs that can localize functionally meaningful clinical effects. Designer neural wavelets hold considerable potential for customizing neural signal and image processing for advanced clinical and experimental applications.

4. ACKNOWLEDGMENT

This work was supported by the US Department of Education. Filter coefficients for the Meyer wavelets used here are available from the first author.

5. REFERENCES

[1] V. J. Samar, K. P. Swartz, & M. R. Raghuveer, *Brain and Cognition, 27, 3,* 398-438 (1995).
[2] S. G. Mallat, *IEEE Trans. on Acoust., Sp, and Sig. Proc., 37(12),* 2091-2110 (1989).
[3.] G. Strang, *Bull. (New Series) of the Am. Math. Soc., 28, 2,* 288-305. (1993)
[4] J. Raz & B. Turetsky, in *Wavelets in Biology and Medicine*, A. Aldroubi and M. Unser, Eds. (in press).
[5] S. J. Schiff, A. Aldroubi, M. Unser, & S. Sato, *Elect. Clin. Neurophys., 91,* 442-455 (1994)
[6] E.A. Bartnik, K.J. Blinowska, & P. J. Durka, *Biological Cybernetics, 67,* 175-181 (1991)
[7] L. J. Trejo, M. J. Shensa, *Proc. of the 1993 Int. Simul. Tech Conf. SIMTEC93/WNN93/FNN93.* San Francisco, Nov 7-10 (1993)
[8] V. J. Samar, G. Kulkarni, K. P. Swartz, I. Parasnis, M. R. Raghuveer, & V. Udpikar, in *Wavelet Applications in Signal and Image Processing II.* A. F. Laine and M. A. Unser, Eds. Proc. SPIE 2303, 496-507 (1994).
[9] S. P. Dear & J. A. Simmons, J. Fritz, *Nature, 364,* 620-623 (1993); S.P. Dear & J. A. Simmons, *Nature* (submitted).
[10] J. O. Chapa & M. R. Raghuveer, *Proc. SPIE Vol. 2491, 518-529, Wavelet Applications II*, H. H. Szu, Ed. (1995).
[11] M. R. Raghuveer & J. O. Chapa, *Proc. SPIE Vol. 2762, 518-529, Wavelet Applications III* (1996).
[12] H. L. Cohen, W. Wang, B. Porjesz, L. Bauer, S. Kuperman, S. J. O'Connor, J. Rohrbaugh & H. Begleiter, *Alcohol, 11, 6,* 583-587 (1994).